Zero-Current Potentials in a Large Membrane Channel: A Simple Theory Accounts for Complex Behavior

Ewa Brygida Zambrowicz and Marco Colombini
Laboratories of Cell Biology, Department of Zoology, University of Maryland at College Park, College Park, Maryland 20742 USA

ABSTRACT Flow of ions through large channels is complex because both cations and anions can penetrate and multiple ions can be in the channel at the same time. A modification of the fixed-charge membrane theory of Teorell was reported (Peng, S., E. Blachly-Dyson, M. Forte, and M. Colombini. 1992. *Biophys. J.* 62:123–135) in which the channel is divided into two compartments: a relatively charged cylindrical shell of solution adjacent to the wall of the pore and a relatively neutral central cylinder of solution. The zero-current (reversal) potential results in current flow in opposite directions in these two compartments. This description accounted rather well for the observed reversal potential changes following site-directed mutations. Here we report the results of systematic tests of this simple theory with the mitochondrial channel, VDAC (isolated from *Neurospora crassa*), reconstituted into planar phospholipid membranes. The variation of the observed reversal potential with transmembrane activity ratio, ionic strength, ion mobility ratio, and net charge on the wall of the pore are accounted for reasonably well. The Goldman-Hodgkin-Katz theory fails to account for the observations.

INTRODUCTION

The mechanisms and laws governing transport processes through biological membranes have been of great interest for many years. One of the simplest membrane transport processes is the flow of molecules and ions through a continuous aqueous pathway formed by a channel-forming membrane protein. Despite its apparent simplicity, the energetics of ion flow through a membrane channel is very complex. Thus experimental results are fitted to theories that greatly simplify the process.

One common assumption is that the aqueous pathway, the pore, is simply a cylinder of bulk solution through which ions traverse by diffusion or under the influence of applied forces. Each ion is assumed to move independently of other ions, guided solely by the local electric field and thermal energy. The local electric field can be approximated either by assuming electroneutrality (Nernst-Planck treatment) or constant field (Goldman-Hodgkin-Katz), although these approximations ignore the structural nature of the pore and any influence the walls of the pore may have on the traversing ions. The shortcomings of these approximations are widely recognized and progress is being made toward theories that take account, in various ways, for the nature of matter within the pore of membrane channels (for examples see: Anderson (1983), Levitt (1991), and Barcilon et al. (1992)).

Fundamental differences exist between ion flow through wide and narrow channels. Ion flow through narrow channels is likely to be dominated by intimate associations between traversing ions and the walls of the channel (binding sites) resulting in high degrees of selectivity. Ion flow through wide channels may be dominated by electrostatic interactions with charges on the walls of the pore. This is not only a reasonable expectation, this is also supported by recent experiments in which the charge on the inner walls of a membrane channel was altered by site-directed mutations. Protein strands forming the walls of the pore were identified by substituting charged residues in these strands by residues of opposite charge (or neutral residues) and looking for changes in selectivity to permeating ions (Blachly-Dyson et al., 1990). The selectivity changes not only identified protein regions close to the stream of permeating ions, but also yielded quantitative clues regarding how charges on the walls of the pore influence ion flow through the pore. It was found that a theory developed by Teorell (Teorell, 1953) to account for ion flow through a fixed-charge membrane could be adapted to describe ion flow through VDAC (Peng et al., 1992). The following paper is intended to be a modest attempt to refine this approach into what will be referred to as the Large-Channel Theory (LCT) and quantitatively test the ability of this theoretical treatment to account for ion flow through VDAC. This simple treatment is adapted to the VDAC channel by using published values for its properties and limited to one adjustable parameter for a poorly estimated property, the net charge on the inner wall of the channel. We found remarkable agreement between this theory and experiments even to the point of describing totally novel phenomenology.

THE VDAC CHANNEL

VDAC (Colombini, 1989; Schein et al., 1976) is a small protein (30 kDa) that forms a large aqueous pore in the mitochondrial outer membrane. Measurements of the Stokes-Einstein radius of the largest nonelectrolyte (Colombini, 1980) that can pass through the channel and electron microscopy of channels after being negatively stained (Mannella, 1982), freeze-dried (Thomas et al., 1991), and frozen in vitreous ice (Mannella et al., 1992), indicate that the channel, in its opened state, forms an aqueous pore about 3 nm in diameter and 5 nm in length (Mannella et al., 1984). The large size of the pore makes it reasonable to expect that

Received for publication 18 August 1992 and in final form 21 May 1993.

0006-3495/93/09/1093/08 $2.00

VDAC's ion selectivity is primarily determined by the electrostatic environment in the pore rather than binding to a site in the wall of the channel. This expectation was supported by selectivity changes following succinylation of the channel (Adelsberger-Mangan and Colombini, 1987) and following the use of site-directed mutation to substitute charged residues with residues of opposite charge (Blachly-Dyson et al., 1990).

MATERIAL AND METHODS

Source of VDAC channels

Mitochondrial membranes were isolated, as previously described (Mannella, 1982) from a log-phase suspension culture of a wall-less mutant of *Neurospora crassa* (ATCC 32360). Isolated mitochondria were lysed by suspending in a hypo-osmotic solution, and the membranes were pelleted at 25,000 × g for 30 min at 4°C. Finally, the membrane pellets were suspended in a solution containing 1 mM KCl, 1 mM Tris-HCl (pH 7.4), and 15% (v/v) dimethyl sulfoxide to a final concentration of approximately 3 mg/ml. The suspension was stored in aliquots at −70°C.

Reconstitution into planar membranes

All experiments were performed on planar phospholipid membranes generated according to the method of Montal and Mueller (1972) as previously described (Colombini, 1987). Membranes were made across a 0.1-mm-diameter hole in a Saran partition separating two buffered salt solutions each at a different concentration. Soybean phospholipids supplemented with cholesterol (1% asolectin, 0.2% cholesterol (Colombini, 1987)) were used to make the membrane. In all experiments the concentration of salt solution at *cis* side of the membrane (as defined below) was higher than the *trans* side (defined below), giving rise to the desired salt gradient. In addition to the salts of interest, each salt solution was supplemented with 2 mM $CaCl_2$ and 0.5 mM morpholinoethanesulfonic acid (MES) (pH 5.8).

Before use, an aliquot of the VDAC preparation was thawed and diluted with buffered salt solution to assure that only moderate numbers of channels were added to the bathing solution. Triton X-100 was added to the VDAC suspension to a final concentration of 1% (v/v), and the mixture was let stand at room temperature for at least 10 min prior to use. After formation of the membrane, 1–20 μl (at lower salt activities, more sample had to be added to obtain the same numbers of channels) of the VDAC-containing solution was added to the solution on the *cis* side of the membrane (4 ml in volume). The solution was stirred during the addition of the VDAC-containing sample, and a low potential was applied (usually −10 mV) to monitor any change in membrane conductance. Insertions of individual channels were observed as stepwise increases in current.

Electrical measurements

An operational amplifier (Analog Devices 50K) in the inverted mode was used to clamp the transmembrane potential (Schein et al., 1976; Colombini, 1987). The membrane current was recorded on chart recorder (Kipp and Zonen BD41). The solution held at virtual ground was defined as the *trans* side thus the signs of potentials refer to the other side, the *cis* side (also the high-salt side). The calomel electrodes were connected to the salt solutions on each side of the membrane by tubings containing the same solution so as to avoid contamination by KCl leaking from the saturated KCl bridge in the electrode. After each experiment the membrane was broken, and the potential needed to bring current to zero was measured (the electrodes dipping into solutions on opposite sides of the membrane). This measured potential is a combination of the electrode asymmetry potential and a liquid junction potential at the hole in the partition separating the two salt solutions. The liquid junction potential was calculated from the standard equation:

$$V_2 - V_1 = \frac{-RT}{F}\frac{u - v}{u + v}\ln\frac{a_2}{a_1}, \quad (1)$$

where, V_2 and V_1 are potentials at the *cis* and *trans* side of the membrane, R, T, and F have their usual meanings, u and v are the cation and anion mobilities, and a_2 and a_1 are the salt activities in the *cis* and *trans* sides of the membrane, respectively. By subtracting the liquid junction potential from the measured potential one gets the actual electrode asymmetry potential. The reversal potential found in each experiment was diminished by the electrode asymmetry potential giving the actual reversal potential due to VDAC selectivity.

An asymmetric triangular voltage wave (5 mHz) was applied to membranes containing one or a few channels. The transmembrane current was recorded. Since VDAC is voltage-gated, the channels opened and closed depending on the applied potential. Care was taken to use the part of the record reflecting current through open channels. The voltage at which this current crossed $I = 0$ (at times extrapolations were needed) was taken as the reversal potential (after correction for electrode asymmetry).

Salt solutions

Salt solutions were prepared in molal concentrations corresponding to the desired activity. Activity coefficients were taken from Robinson and Stokes (1959). In the case of acetic acid salts: CH_3COONa and CH_3COOK, solutions corresponding to 0.6 and 0.06 activities were prepared. Subsequently, these activities values were corrected for metal complexation (Smith and Martell, 1976) yielding actual activities of dissociated ions as follows: for CH_3COONa, 0.44 and 0.06 giving rise to a 7.4-fold gradient, and for CH_3COOK, 0.46 and 0.06 giving rise to 7.7-fold gradient.

RESULTS AND DISCUSSION

The theory developed by Peng and coworkers (Peng et al., 1992) (see Theory section) separates the aqueous pore, formed by the membrane channel, into two compartments (Fig. 1) a charged cylindrical shell of solution and a central neutral cylinder. For the current study, we refined the theory in two ways: i) We defined the limits of the cylindrical shell as the distance (critical distance) at which the surface potential decayed to $1/e$ of its value at the surface (this length is equivalent to the Debye length in Gouy/Chapman theory). We derived an equation to determine this distance for the inside of a hollow cylinder (see Appendix). The critical distance calculated for the two ends of the channel was averaged to obtain the effective critical distance for the entire channel; ii) The size of the ions was included by subtracting the radius of the anion from the thickness of each compartment (because the experiments were performed on a channel that has a net positive charge on its wall, anions are more likely to collide with the sides of the wall). This relatively crude theory accounted quite well for the changes in reversal potential of VDAC with changing net charge within the pore (Peng et al., 1992).

Here we tested this "Large-Channel Theory" by determining how well it could account for the zero-current potentials produced under a variety of conditions: 1) two- to 20-fold ion activity gradients; 2) varying ionic strength; 3) using ions with different mobilities; and 4) varying the charge on the wall of the channel (experimental data from the literature but with the theoretical curve using the above refinements). Experiments were performed on membranes containing only

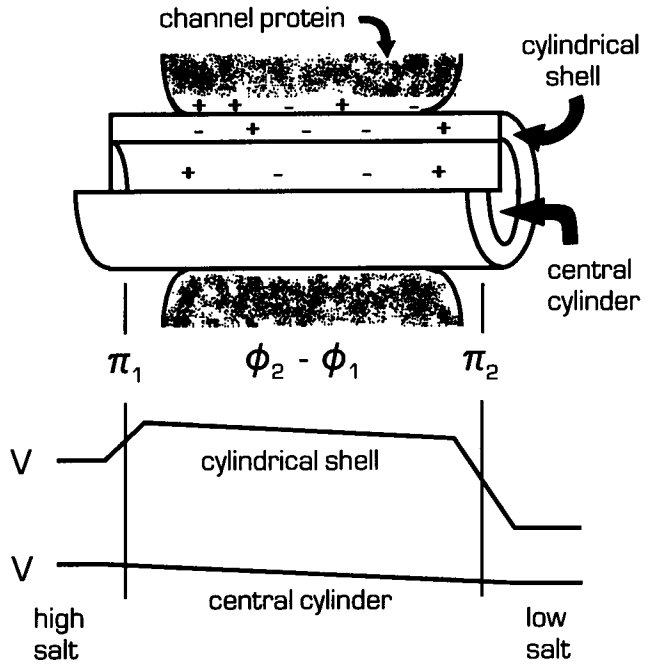

FIGURE 1 Schematic representation of the partitioning of the aqueous pore into two compartments and the electrical potential profile in each. The net charge on the inner wall of the channel results in a cylindrical layer of charged solution next to the protein (the cylindrical shell). The thickness of this shell is proposed to be a mean of the critical distances calculated for the ionic strength at each end of the channel. The central cylinder is therefore relatively neutral. The cylinders of solution extend beyond the end of the protein because of access resistance regions. The electrical potential changes along the cylindrical shell are the two Donnan potentials at the ends of the pore (π_1 and π_2) and the diffusion potential ($\phi_2 - \phi_1$) in the pore. Donnan potentials do not apply to the central cylinder.

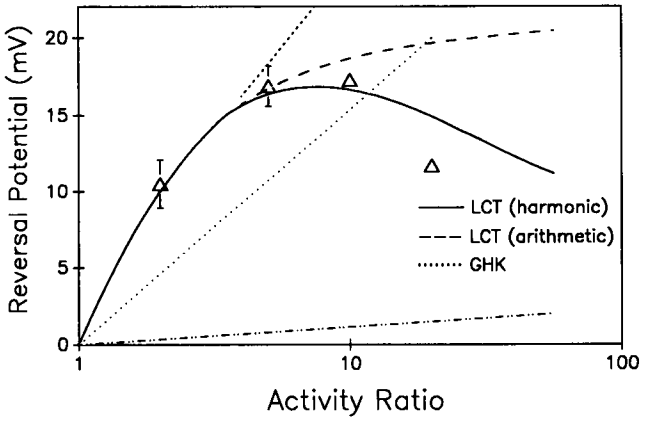

FIGURE 2 Variation of VDAC's reversal potential with the transmembrane activity ratio of KCl. Experimental measurements made in the presence of 2-, 5-, 10-, and 20-fold KCl activity gradients (activity of the low side was kept constant at 0.06) were 10.5 ± 1.6 mV (3), 16.9 ± 1.3 mV (5), 17.3 ± 0.5 mV (3), 11.7 ± 0.2 mV (3). Values were ± standard deviation, with number of experiments in parentheses. The error bars on some of the experimental data are smaller than the symbols. The curves are predictions of the LCT (*solid* and *line* with *wide dashes*) and the straight line prediction of Goldman-Hodgkin-Katz (GHK) (*dotted line*). The slope of the GHK line is arbitrary. Also illustrated are the calculated reversal potentials of the cylindrical shell (*narrow dashes*) and the central cylinder (–··–··).

one or few channels inserted, in order to have confidence that all observations were made on channels in their open state. Reversal potentials were measured repeatedly, and an average value was used as a single estimate for that one experiment.

In the theoretical calculations of the reversal potential under experimental conditions 1), 2), and 3), the net charge on the walls lining the aqueous pore of VDAC was assumed to be positive 3.5. This estimate for *N. crassa* VDAC is close to that estimated for yeast VDAC (+2.5 (Blachly-Dyson et al., 1990)) and allowed the data to fit better to the theory. This is the only parameter that was adjusted.

REVERSAL POTENTIAL AS A FUNCTION OF SALT ACTIVITY RATIO

The reversal potential of VDAC channels incorporated into planar phospholipid membranes was measured in the presence of 2-, 5-, 10-, and 20-fold potassium chloride activity gradients across the membrane. The activity of the *trans* side solution was maintained at 0.06, while the *cis* side was varied: 0.12, 0.30, 0.60, and 1.2. Fig. 2 compares the measured values to three theoretical curves: the straight line predicted by the Goldman-Hodgkin-Katz equation (GHK, *dotted line*) and two curves representing two versions of the LCT.

The LCT uses a two-compartment model to represent the ionic solution within the channel (Fig. 1). The cylindrical shell containing the fixed charge on the inner wall of the protein has a calculated reversal potential given by the curve with the short dashes. The calculated reversal potential of the central cylinder is given by the line of alternating dots and dashes. The effective reversal potential of the channel (*solid* and *wide-dashed line*) are given by a combination of the two. The "critical distance" is used to define the thickness of the cylindrical shell of solution adjacent to the charged wall of the pore. Different salt activities in the bulk phases at the two ends of the channel result in different calculated critical distances. For simplicity these are combined to yield a compromise critical distance by either using the arithmetic mean (*dashed line*) or the harmonic mean (*solid line*). These means differ significantly only at large activity ratios. The harmonic mean favors the lower value and does a better job in following the experimental observations.

The major difference between the classical GHK theory and LCT in accounting for the data in Fig. 2, is the biphasic nature of the latter theory. According to LCT, the potential generated by the outer compartment, the cylindrical shell, depends on the Donnan potentials at the ends of the channel and the diffusion potential of the mobile ions in the channel. For KCl, the diffusion potential is small because the mobilities of K^+ and Cl^- are very close (7.62×10^{-4} and 7.92×10^{-4} $cm^2\ s^{-1}V^{-1}$, respectively (Robinson and Stokes, 1959)). Thus the Donnan potentials dominate the reversal potential of this compartment. The reversal potential of the central cylinder depends solely on the diffusion potential. Under the experimental conditions of Fig. 2, the reversal potential of the central cylinder was very close to zero. As a result, the central cylinder acted as a shunt, reducing the overall calculated

reversal potential. (This is not the case for salts composed of ions with quite different mobilities.) As the activity ratio increases, the critical distance in the high-salt side declines resulting in a greater proportion of the current passing through the central, cylindrical compartment. Thus, the expected increase in reversal potential with increasing KCl activity gradient was diminished by changes in the thickness of the charged shell. At the calculated reversal potential the theory predicts that current is flowing in opposite directions in the two regions of the channel.

The reversal potentials measured in the presence of 2-, 5-, and 10-fold KCl activity gradients fit the predictions of LCT rather well, especially when the harmonic mean was used. However, the reversal potential measured in the presence of the 20-fold KCl gradient indicates a more rapid drop with activity ratio than predicted by LCT. The large KCl activity gradient was accompanied by a large osmotic gradient (3.8 osmol/kg difference in osmotic pressure (Robinson and Stokes, 1959)). The possibility that water flow through the channel might affect the measurements (Rosenberg and Finkelstein, 1978; Levitt et al., 1978), was tested by supplementing the low salt solution with 2.75 M glycerol.[1] The reversal potential obtained in this experiment was the same as in the absence of glycerol. Additionally reversal potential was measured in 0.6 vs. 0.03 KCl activity gradient. Experimental data (not shown) also deviated substantially from the theoretical calculations. Clearly, the two-compartment approach is deficient at high activity ratios.

Reversal potential as a function of ionic strength

In these experiments the KCl activity ratio was maintained at 2.0. Three pairs of solutions were tested: 0.06 vs. 0.03, 0.12 vs. 0.06, and 1.2 vs. 0.6. GHK theory predicts the same reversal potential in all three cases, but LCT predicts a decline in reversal potential as the critical distance declines.

Fig. 3 shows good agreement between the measurements and the theory at intermediate and high salt activities but substantial deviation at low salt. Below an activity of 0.1 on the low-salt side, the critical distance is longer than the channel radius for the solutions on both sides of the membrane. The central compartment vanishes, and the reversal potential is given solely by one charged compartment. This clearly overestimates the reversal potential of the channel. Nevertheless, LCT works well at physiological salt concentrations and above.

Reversal potential as a function of ion mobility ratio

The experiments described in the Materials and Methods were performed using KCl as the salt. According to LCT, with KCl the cylindrical shell is primarily responsible for the elevated reversal potential, while the central cylinder acts as a shunt. However, the use of salts with rather different mobilities can change the situation rather markedly. Since VDAC shows some selectivity for anions over cations, choosing a salt with a more mobile anion should augment the measured reversal potential. The converse would occur with a less mobile anion.

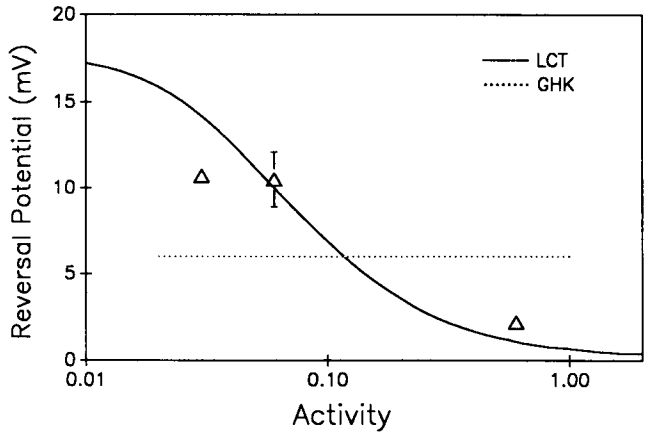

FIGURE 3 Variation in VDAC's reversal potential with ionic strength of KCl in the solution. The reversal potential is plotted against the activity of the low-salt side. The activity ratio was kept constant at 2.0. The error bars reflect the standard deviation and when not included were less than the size of the symbol. The solid line is the calculation using LCT and the harmonic mean of the critical distances at the two ends of the channel. The position of the zero-slope line predicted by GHK (*dotted line*) is arbitrary.

Salts were chosen so as to obtain a wide range of mobilities of the cation to the anion but restricted to salts where activity measurements are available. The reversal potential of VDAC was tested in the presence of 10-fold activity ratios (0.6 vs. 0.06) for LiCl, NaCl, NH_4Cl, and KCl. Similar experiments were performed with sodium acetate and potassium acetate at the same total activity. The reported activity ignores complexation between the ions resulting in neutral species in solution (Smith and Martell, 1976). By correcting for the complexes we estimate activity ratios of the dissociated sodium and potassium acetate to be 7.4 and 7.7, respectively.

As illustrated in Fig. 4, the change in reversal potential with activity ratio occurred as expected. However, the agreement between theory and experiment diminishes as the mobility ratio moves away from 1. LCT predicts a greater effect of diffusion potentials within the channel than observed. An increase in the size of the ions due to hydration might account for part of this.

Reversal potential as a function of net charge in the channel

The experimental data plotted here was taken from published work (Blachly-Dyson et al., 1990; Peng et al., 1992). Site-directed mutations that influenced the selectivity of VDAC are likely to be located near the ions flowing through the channel. In addition, an analysis of the primary sequence (Blachly-Dyson et al., 1989) placed these sites on the wall

[1] The addition of glycerol to balance the osmotic pressure due to the salt gradient introduces other problems. It affects the salt activity. The large size of VDAC's pore allows ions and glycerol to flow through. Thus working out the flow of solution through the pore is no simple matter. In any case, the lack of effect of the added glycerol indicates that osmotic flow has little effect.

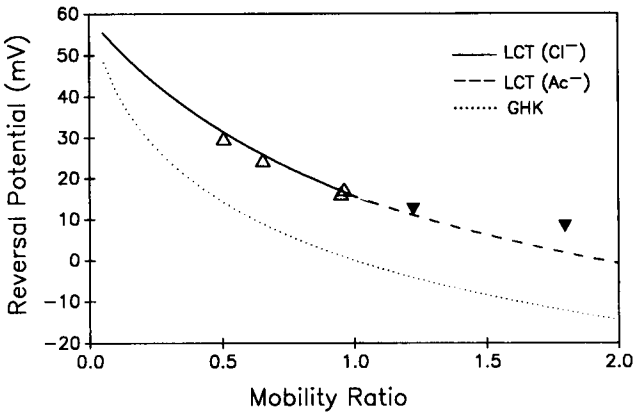

FIGURE 4 Variation of VDAC's reversal potential with the mobility ratio (anion/cation) of the ions in the medium. Reversal potentials measured in the presence of 10-fold LiCl, NaCl, NH_4Cl, and KCl activity gradients were 29.9 ± 1.6 mV (6), 24.5 ± 1.1 mV (4), 16.3 ± 0.3 mV (3), 17.3 ± 0.5 mV (3), resp. 7.4-fold sodium acetate, and 7.7-fold potassium acetate activity gradient yielded reversal potentials 12.3 ± 1.0 mV (4), and 8.3 ± 1.1 mV (6), respectively. Data were mean value ± standard deviation with number of experiments given in parentheses. The solid line is the LCT prediction for the chloride salts. The dashed line is for potassium acetate (the curve for sodium acetate was almost the same). The GHK prediction (*dotted line*) is based on using ionic mobilities for permeabilities in the equation.

lining the channel's aqueous pore. Thus, for the purpose of testing LCT, mutations that influenced VDAC's ion selectivity are assumed to alter the net charge on the walls of the channel by an amount equivalent to the engineered charge change. Since the data were collected using yeast VDAC, in plotting the data we assume a net charge in the wild-type VDAC channel of +2.5 (the same charge as proposed by the original investigators (Peng et al., 1992)).

In Fig. 5, the curve is the prediction from LCT using critical distance and the harmonic mean. Unlike the previous

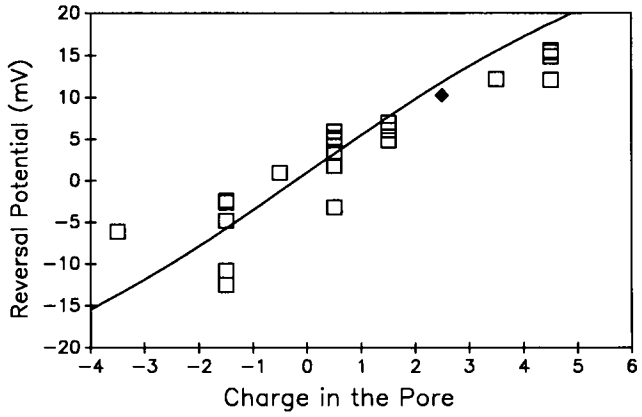

FIGURE 5 Variation in channel reversal potential with the net charge on the protein wall lining the aqueous pore. The data points are the measured reversal potentials for yeast VDAC. The values for wild-type VDAC (*diamond*) and VDAC mutants with engineered point mutations (*squares*) were taken from previous publications (Blachly-Dyson et al., 1990; Peng et al., 1992). Experiments had been performed in the presence of 1.0 M KCl vs. 0.10 M KCl (activity ratio of 7.8) with 5.0 mM $CaCl_2$ and 1.0 mM MES (pH 5.8) present on both sides. The solid line is that calculated from LCT using the harmonic mean.

theoretical treatment (Peng et al., 1992), the thickness of the charged shell was not given a reasonable value but calculated as the critical distance from the existing ion activities. While the fit is not as good, especially at high positive charge in the pore, the correlation with the data is quite reasonable in view of the simplicity of the approach. No attempt was made to address the location of the charge change or the lack of uniformity in the charge distribution.

Conclusions

A relatively simple theory can account qualitatively and often quantitatively for the often complex way in which the reversal potential measured in VDAC channels varies with the ionic and charged environment within the channel. While it would surprise no one that the reversal potential would not increase indefinitely with increasing salt activity ratio, a pronounced decline seems unexpected. LCT predicted this decline by dividing the aqueous space within the pore into two compartments each with its own reversal potential. The combined reversal potential thus results in current moving in opposite directions in the two compartments. Since the properties of the two compartments and their relative contributions to the overall reversal potential vary with the activity ratio, the biphasic dependence is expected. Similarly, the agreement between experiment and theory with variation in ion mobility, ionic strength, and total charge in the channel can be traced to the use of this two-compartment model. A more sophisticated model that accounts for the continual change in potential with distance from the walls of the channel may work better. However, the roughness of the surface of the protein wall, the uneven distribution of charge, and the change in properties with distance through the channel, may all need to be addressed to obtain a more accurate theoretical treatment. Clearly the lack of detailed structural information hampers the formulation of a detailed description of the properties of the channel.

A consequence of LCT is that the reversal potential should increase as the channel radius is decreased without any change in the net charge on the wall of the channel. This should still hold if the charge density in the cylindrical shell were kept constant, while the overall radius of the pore was reduced. These predictions are hard to test by direct experiment but were verified indirectly by changing the ionic strength and thus the fraction of the pore volume that comprised the cylindrical shell.

The quantitative agreement between theory and experiment is remarkable especially since the theory used only one adjusted parameter, the net charge in the pore. This parameter could not have any value. Work on yeast VDAC showed that the net charge was about +2.5. We found that +3.5 worked better for *N. crassa*. All other information came from the literature.

The results were compared with the predictions made from the Goldman-Hodgkin-Katz equation. The large size of the channel and its ability to allow both cations and anions to cross the membrane makes it unlikely that ions are moving through the membrane independently thus violating one of

the premises of GHK theory. However, GHK does not consider the properties of the protein wall. This is the biggest drawback and probably the reason why GHK fared so poorly in its ability to account for the qualitative aspects of the data, much less make any quantitative predictions.

The LCT presented here should not be limited to accounting for the properties of VDAC. It should fare well with any protein forming a large aqueous pore. In using this theory with channels about which much less is known, it may be possible to gain important information such as pore size and net charge within the pore by fitting to this theory.

APPENDIX: A SIMPLE THEORY OF ION FLOW THROUGH LARGE CHANNELS

As previously published (Peng et al., 1992), the large-channel theory applies the fixed-charge membrane theory of Teorell to a portion of the ion flow through the channel.

i) The fixed-charge theory of Teorell

A theory of ion flow through a membrane consisting of a matrix of fixed charges was published by Torsten Teorell in 1953. It assumes the following experimental conditions:

1. The membrane is a thin sheet separating two aqueous compartments. It is composed of a matrix of fixed charges in an aqueous environment. Mobile ions flow through the water-filled spaces between the fixed charges. The membrane is homogeneous throughout with regard to fixed charges and water-filled spaces so that one may define a membrane "fixed-charge concentration."

2. All ions are regarded as permeable through the membrane with mobilities equal to "bulk-phase" mobilities.

3. Donnan equilibria exist at each membrane-water interface determining the concentration of free ions at the membrane surfaces. Ion flow through the membrane is determined by thermal motion, ion mobilities, and any potential difference between the two membrane surfaces.

With these assumptions Teorell derived an expression for the total membrane potential as equal to the sum of two Donnan potentials at the membrane boundaries and a Nernst-Planck diffusion potential within the membrane. Although Teorell derived a general flux equation, for the purpose of this paper we focused on the special case: a single monovalent salt under zero-current conditions. The reversal (zero-current) potential (E) is related to the fixed-charge concentration in the membrane, the mobilities of the individual ions, and the salt concentration gradient.

$$E = \pi_1 + \pi_2 + (\phi_2 - \phi_1) \tag{2}$$

where π_1 is the Donnan potential between the solution at side 1 and the membrane surface at side 1; π_2 is the Donnan potential between the membrane surface at side 2 with the solution at side 2; $(\phi_2 - \phi_1)$ is the diffusion potential within the membrane. See the electrical potential profile for the cylindrical shell in Fig. 1.

The Donnan potential π, is given by:

$$RT/F \ln r \tag{3}$$

where R is the gas constant, F is the Faraday constant, T the absolute temperature, and r is the Donnan ratio. The Donnan ratio is determined by the fixed-charge concentration in the membrane (X) and the bulk phase salt activities, a, in the solution:

$$r = \sqrt{1 + \left(\frac{X}{2a}\right)^2} - \frac{X}{2a}. \tag{4}$$

The diffusion potential within the membrane is

$$\phi_2 - \phi_1 = \frac{u - v}{u + v}\frac{RT}{F} \ln \frac{a_1\left(r_1 u + \frac{v}{r_1}\right)}{a_2\left(r_2 u + \frac{v}{r_2}\right)}, \tag{5}$$

where u and v are the mobilities of the cation and anion, respectively, and other symbols are as above. Combining Eqs. 2, 4, and 5 (note: the two Donnan potentials are opposite in direction) yields an equation for zero-current potential across the membrane:

$$E = \frac{RT}{F} \ln\left(\frac{r_2}{r_1}\right) + \frac{u - v}{u + v}\frac{RT}{F} \ln \frac{a_1\left(r_1 u + \frac{v}{r_1}\right)}{a_2\left(r_2 u + \frac{v}{r_2}\right)}. \tag{6}$$

ii) Modifications for large channels: the large-channel theory

Two-compartment model

A major assumption in Teorell's theory is the homogeneous distribution of the fixed charge in the membrane. Since, in a channel, charges on the wall will extend only a short distance from the wall, Teorell's theory should only apply to a shell of solution close to the wall of the channel (Fig. 1). Perhaps a reasonable estimate for the thickness over which the surface potential decays to $1/e$ of its value at the surface, here referred to as the critical distance. For planar geometry this would be 1 Debye length (Gouy-Chapman theory). The core of the channel would then be equivalent to an uncharged cylinder of water. These two pathways would be in parallel and each have their own characteristics combining to yield the characteristics of the channel as a whole.

The critical distance inside a charged cylinder

The electrical potential (V) in an electrolyte solution filling the inside of a uniformly charged hollow cylinder of infinite length is given by

$$\frac{d^2V}{dr^2} + \frac{1}{r}\frac{dV}{dr} + \frac{2F^2IsV}{\epsilon\epsilon_0 RT} \tag{7}$$

where Is is the ionic strength; $\epsilon\epsilon_0$ is the permittivity of the solution in the cylinder; r is the distance from the center of the cylinder; and the other symbols have their usual meanings. Note that Eq. 7 has been simplified by assuming that the potential does not vary in the "z" direction (direction perpendicular to the membrane). This differential equation can be solved to yield

$$\frac{V}{V_0} = \frac{1 + \frac{Xr^2}{4} + \frac{X^2r^4}{64} + \frac{X^3r^6}{2304} + \frac{X^4r^8}{147456} + \frac{X^5r^{10}}{14.74 \times 10^6} + \cdots}{1 + \frac{Xr_0^2}{4} + \frac{X^2r_0^4}{64} + \frac{X^3r_0^6}{2304} + \frac{X^4r_0^8}{147456} + \frac{X^5r_0^{10}}{14.74 \times 10^6} + \cdots} \tag{8}$$

where

$$X = \frac{2F^2Is}{\epsilon\epsilon_0 RT} \tag{9}$$

V_0 is the potential at the surface of the charged cylinder and r_0 is the radius of the cylinder.

The "critical distance" in the cylinder is defined as the distance from the surface at which the potential decays to $1/e$ of that at the surface. Fig. 6 shows a comparison of the way in which the potential decays with distance from the inner surface of the cylinder (1.5-nm inside radius) as determined by Eq. 8 (*solid line*) as compared to the classical calculation for planar geometry (*dotted line*). For this large channel, the two geometries yield similar results

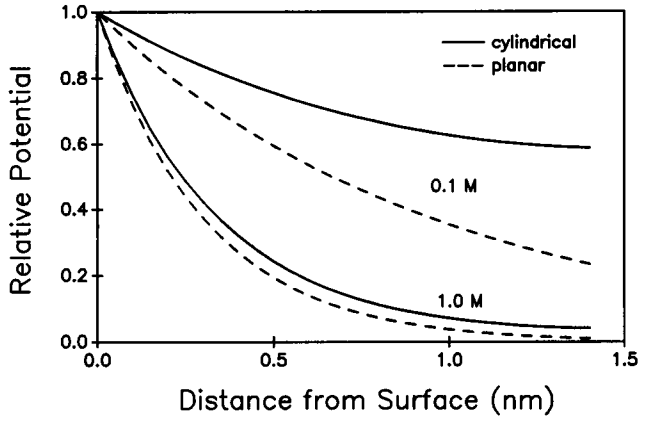

FIGURE 6 The decay of electrical potential with distance from a positively charged surface. Dotted lines are for a flat charged surface in an aqueous solution with the indicated ionic strength. The solid lines are for the inner surface of a hollow cylinder, of internal radius 1.5 nm, filled with an aqueous solution of the indicated ionic strength.

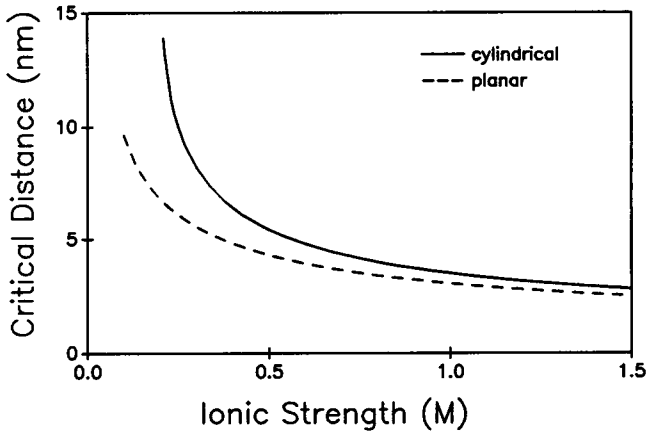

FIGURE 7 Critial lengths for planar (*dotted line*) and cylindrical (*solid line*) geometries as a function of the ionic strength of the aqueous medium. The critical distance is defined as the distance from the surface at which the electrical potential has decayed to $1/e$ of the value at the surface. This length was determined for relations such as those shown in Fig. 6.

in the presence of 1.0 M salt but quite different results for 0.1 M salt. Clearly, as the critical distance approaches the radius of the channel, its value is strongly influenced by the local geometry. This is also evident from the relationship between critical distance and ionic strength (Fig. 7) for planar (*dotted line*) and cylindrical (*solid line*) geometries. Thus, the critical distance was used for all subsequent theoretical calculations.

Theoretical estimate of the reversal potential

The reversal potential of the channel was taken to be a weighted average of the reversal potential of the charged cylindrical shell and the relatively neutral central cylinder. Equations 2 through 6 were used to calculate the reversal potential of the charged cylindrical shell. Literature data was used for all calculations except for the net charge on the wall of the pore (allowed to vary because it is not known to sufficient precision). The overall pore size radius is 1.5 nm and its length is 5 nm. For the uncharged central cylinder, the same equations were used except that the Donnan ratios (r) were set equal to 1. The weighting used was the fractional cross-sectional area of each compartment. The thickness of the charged shell was approximated by the mean value of the critical distance for solutions on each side of the membrane. Both the arithmetic and harmonic means are considered. The radii of both the pore and the central cylinder were reduced by the radius of the anion penetrating the channel. The ionic radii[2] for chloride and acetate were taken as 0.18 (Ladd, 1968) and 0.22[2] nm, respectively. The radius of the circle forming the cross-sectional area of the central cylinder is the radius of the pore minus the critical distance (minus the ionic radius).

The effective length of the pore is longer than the physical length because of the access resistance. Phenomena resulting from this access resistance have been reported for VDAC (Mangan and Colombini, 1987). We applied the theory of Hall (1975) to determine this effective length. The length of the channel was increased by 0.8 times its diameter. The diameter of VDAC's pore is estimated at 3 nm, and its length at 5 nm. Therefore the effective length is 7.4 nm.

[2] The radii of the anions was chosen because these would be higher in concentration next to the wall of the channel and thus would be most subject to steric restrictions. Hydrated radii were not used, because, while there are good estimates for hydration of chloride (four water molecules), to our knowledge such is not the case for acetate. For acetate we estimated the ionic radius by taking half the geometric mean of the dimensions of the smallest rectangular box containing a space-filling model of the molecule. This was estimated to be 0.5 × 0.45 × 0.4 nm.

It is clearly contradictory to, at once, assume a Donnan equilibrium at the channel openings and to invoke an access resistance region. Yet, to ignore the access resistance in order to be consistent in assuming equilibrium at the channel openings flies in the face of reality (see Mangan and Colombini (1987)). Thus, the channel must be effectively longer due to the access resistance and the use of Hall's theory to estimate the increased length seems a reasonable approach.

We thank Prof. Maciej J. Nalecz of the Nencki Institute in Warsaw for initiating and facilitating E. B. Zambrowicz's extended visit to the University of Maryland at College Park. This work was supported by the Office of Naval Research grant N00014–90-J-1024 and National Institutes of Health grant GM 35759. During this work E. B. Zambrowicz was supported with a fellowship from the Kosciuszko Foundation.

REFERENCES

Adelsberger-Mangan, D. M., and M. Colombini. 1987. The elimination and restoration of voltage dependence on the mitochondrial channel, VDAC, by graded modification with succinic anhydride. *J. Membr. Biol.* 98:157–168.

Anderson, O. S. 1983. Ion movement through gramicidin A channels: interfacial polarization effects on single-channel current measurements. *Biophys. J.* 41:135–146.

Barcilon, V., D.-P. Chen, and R. S. Eisenberg. 1992. Ion flow through narrow membrane channels: Part II. *Siam J. Appl. Math.* 52:1405–1425.

Blachly-Dyson, E., S. Z. Peng, M. Colombini, and M. Forte. 1990. Alteration of the selectivity of the VDAC ion channel by site-directed mutagenesis: implications for the structure of a membrane ion channel. *Science.* 247:1233–1236.

Blachly-Dyson, E., S. Z. Peng, M. Colombini, and M. Forte. 1989. Probing the structure of the mitochondrial channel, VDAC, by site-directed mutagenesis: a progress report. *J. Bioenerg. Biomembr.* 21:471–483.

Colombini, M. 1987. Characterization of channels isolated from plant mitochondria. *Methods Enzymol.* 148:465–475.

Colombini, M. 1980. Structure and mode of action of a voltage-dependent anion-selective channel (VDAC) located in the outer mitochondrial membrane. *Ann. N. Y. Acad. Sci.* 341:552–563.

Colombini, M. 1989. Voltage gating in the mitochondrial channel, VDAC. *J. Membr. Biol.* 111:103–111.

Hall, J. E. 1975. Access resistance of a small circular pore. *J. Gen. Physiol.* 66:531–532.

Ladd, M. F. C. 1968. The radii of spherical ions. *Theoret. Chim. Acta.* 12:333–336.

Levitt, D. G., S. R. Elias, and J. M. Hautman. 1978. Number of water molecules coupled to transport of sodium, potassium and hydrogen ions via gramicidin, nonactin or valinomycin. *Biochim. Biophys. Acta.* 512: 436–451.

Levitt, D. G. 1991. General continuum theory for multiion channel. I. Theory. *Biophys. J.* 59:271–277.

Mangan, P. S., and M. Colombini. 1987. Ultrasteep voltage dependence in a membrane channel. *Proc. Natl. Acad. Sci. USA.* 84:4896–4900.

Mannella, C. A., M. Radermacher, and J. Frank. 1984. Three-dimensional structure of mitochondrial outer-membrane channels from fungus and liver. Proc. 42nd Ann. Meet. EMSA. G. W. Bailey, editor. San Francisco Press, San Francisco. 644–645.

Mannella, C. A. 1982. Structure of the outer mitochondrial membrane: ordered arrays of pore-like subunits in outer-membrane fractions from *Neurospora crassa* mitochondria. *J. Cell Biol.* 94:680–687.

Mannella, C. A., M. Forte, and M. Colombini. 1992. Toward the molecular structure of the mitochondrial channel, VDAC. *J. Bioenerg. Biomembr.* 24:7–19.

Montal, M., and P. Mueller. 1972. Formation of bimolecular membranes from lipid monolayers and a study of their electrical properties. *Proc. Natl. Acad. Sci. USA.* 69:3561–3566.

Peng, S., E. Blachly-Dyson, M. Forte, and M. Colombini. 1992. Large scale rearrangement of protein domains is associated with voltage gating of the VDAC channel. *Biophys. J.* 62:123–135.

Robinson, R. A., and R. H. Stokes. 1959. Electrolyte Solutions. Butterworths, London.

Rosenberg, P. A., and A. Finkelstein. 1978. Interaction of ions and water in gramicidin A channels: streaming potentials across lipid bilayer membranes. *J. Gen. Physiol.* 72:327–340.

Schein, S. J., M. Colombini, and A. Finkelstein. 1976. Reconstitution in planar lipid bilayers of a voltage-dependent anion-selective channel obtained from *Paramecium* mitochondria. *J. Membr. Biol.* 30:99–120.

Smith, R. M., and A. E. Martell. 1976. Critical Stability Constants Volume 4: Inorganic Complexes. Plenum Press, New York.

Teorell, T. 1953. Transport processes and electrical phenomena in ionic membranes. *Prog. Biophys. Biophys. Chem.* 3:305–369.

Thomas, L., E. Kocsis, M. Colombini, E. Erbe, B. L. Trus, and A. C. Steven. 1991. Surface topography and molecular stoichiometry of the mitochondrial channel, VDAC, in crystalline arrays. *J. Struct. Biol.* 106:161–171.